Deadtime correction for two multihead Anger cameras in ^{131}I dual-energy-window-acquisition mode

Kenneth F. Koral, Kenneth R. Zasadny, Robert J. Ackermann, and Edward P. Ficaro
Internal Medicine, Division of Nuclear Medicine, The University of Michigan Medical Center, Ann Arbor, Michigan 48109

(Received 15 April 1996; accepted for publication 13 October 1997)

Two side-by-side energy windows, one at the photopeak and one at lower energy, are sometimes employed in quantitative SPECT studies. We measured the count-rate losses at moderately high activities of ^{131}I for two multihead Anger cameras in such a dual-window-acquisition mode by imaging a decaying source composed of two hot spheres within a warm cylinder successively over a total of 23 days. The window locations were kept fixed and the paralyzable model was assumed. In addition, for the Picker Prism 3000 XP camera, the source was viewed from three different angles separated by 120° and the final results are from an average over these three angles. For the Picker camera, the fits to the data from the individual windows are good (the mean of the squared correlation coefficient equals 0.98) while for the Siemens Multispect camera fits to the data from head 1 and from the lower-energy, monitor window are relatively poor. Therefore, with the Siemens camera the data from the two windows are combined for deadtime computation. Repeated autopeaking might improve the fits. At the maximum count rate, corresponding to a total activity of 740 MBq (20 mCi) in the phantom, the multiplicative deadtime correction factor is considerably larger for the Picker than for the Siemens camera. For the Picker camera, it is 1.11, 1.12, and 1.12 for heads 1–3 with the photopeak window and 1.10 for all heads with the lower-energy monitor window. For the Siemens camera, the combined-window deadtime correction factor is 1.02 for head 1 and 1.03 for head 2. Differences between the deadtime correction factor for focal activity and for the total activity do not support the hypothesis of count misplacement between foci of activity at these count rates. Therefore, the total-image dead time correction is recommended for any and all parts of the image.
[S0094-2405(98)00301-0]

Key words: deadtime, Anger camera, ^{131}I, SPECT, scatter

I. INTRODUCTION

At the University of Michigan, Anger-camera dual-energy-window-acquisition mode is utilized in an algorithm designed to yield accuracy in focal quantification for patients being monitored during ^{131}I radioimmunotherapy.[1] From the lower-energy window, one derives an estimate of the number of corrupting gamma rays that are included within the higher-energy window. This value can then be subtracted from the counts in that window.[2] With ^{131}I, the correction has to account for the perturbation of the expected count due to patient Compton scattering of the primary 364 keV gamma ray and also due to energy degradation of higher-energy emissions (637, 713 keV, etc.). This degradation presumably occurs through (1) patient Compton scattering, (2) collimator Compton scattering, (3) collimator septal penetration coupled with partial energy deposition in the crystal, or (4) combinations of the above.[3–5] Complicating matters, imaging therapy patients after the administration of a large amount of ^{131}I radioactivity can lead to significant losses of counts due to camera deadtime.[1] One group has employed lead attenuation sheets between the patient and camera to reduce the camera count rate.[6] We employ a deadtime correction for the moderate levels of radioactivity present at the time of our imaging: less than an estimated 30 mCi (1110 MBq) total body burden.

Previous efforts by others[7–17] have modeled the dead time behavior of Anger cameras for radioisotopes with a single energy window at high counting rates. The camera dead time has been shown to be dependent on the scattering condition in the source. The reason: count rates from a single photopeak window do not account for photons having other energies. These photons do contribute significantly to the dead time of the camera electronics.

We have previously[18] measured the deadtime losses of a General Electric 400 AT Anger camera in the dual-energy-window-acquisition mode for clinical situations where dead time losses are at a fairly low level ($\leqslant 25\%$). That research is now extended to two multihead Anger cameras likely to be employed in quantitative imaging of new patients. (Both cameras have heads with 9.5 mm thick crystals.) Our goal is to obtain a correction factor for dead time that will be sufficiently accurate so as to contribute little to an overall quantitative uncertainty of 10% for activity. In the new research, we (1) employ the paralyzable model and use the decaying source method, (2) initially treat the data from each window separately in obtaining a dead time-correction factor, F, (3)

compare the results from different heads, and (4) look into the dependence of the correction on the geometry of the phantom being imaged.

In addition, at higher count rates, Ceeburg and Strand have reported that events may be mispositioned in the image even if they are not lost altogether.[19] When there are two or more high-activity foci, they report that counts are misplaced along the lines that join the high-activity locations. To investigate the possibility of count misplacement for our cameras and at our count rates, we (1) choose our phantom to have both focal and distributed radioactivity, (2) compute a dead time constant for not only the total image but also for only the counts within a region of interest (ROI) covering the projection of the focal activity, and (3) compare the values of the dead time correction factor for the focal activity and for the total activity.

II. THEORY

To review the theory, the dead time correction factor, F, can be defined to correct the observed count rate, N', to produce an estimate of the true count rate, N,

$$N = FN'. \tag{1}$$

Here, the observed count rate is that found in the image recorded by the computer attached to the gamma camera.

With the paralyzable model,

$$N' = Ne^{-N\tau}, \tag{2}$$

where τ is the dead time constant. Furthermore, it can easily be shown[20] that for a decaying source that has a disintegration constant, λ, and that is measured at time, t, $\lambda t + \ln N'$ can be plotted against $e^{-\lambda t}$ and τ can be related to the slope and intercept of the best fit to that data by

$$\tau = -(\text{slope})e^{-\text{intercept}}. \tag{3}$$

The relationship [from Eqs. (1) and (2)] between the observed count rate N' and the paralyzable-model dead time correction factor F is

$$F = e^{N'\tau F}. \tag{4}$$

One can solve for F for a given N' and τ by iteration. That is, one guesses a value for F and then checks if it is consistent with Eq. (4) for the given N' and τ. If not, it is varied until the equation is satisfied.

III. METHODS

A cylindrical, water-filled phantom of an elliptical cross section containing two 6-cm-diam, water-filled spheres was used to approximate the scattering conditions that would be encountered while imaging tumors in a patient. The long axis inside dimension of the ellipse measured 30.4 cm and the short axis 21.9 cm. This cross section approximates that seen in patient body imaging. The inside height of the phantom was 17.8 cm. The spheres were symmetrically placed on the long axis, the centers 8.6 cm away from the ''center'' of the elliptical cross section and 10.2 cm from the bottom (nonlip end) of the cylinder. Symmetry was maintained to aid in the interpretation of data obtained with a camera head that was rotated 120° from its standard position. Requiring this symmetry argued against a more lifelike but less symmetric phantom. The phantom was successfully imaged nine times over 23 days with the Siemens camera and at 8 of those times with the Picker camera. The times were chosen so that the difference in the count rate between successive acquisitions was approximately the same. As the source activity decayed, imaging time was increased from 30 to 180 s so that the counting statistics for each image were about the same. For the first acquisition, the entire phantom contained 740 MBq (20 mCi) with the spheres having equal activity and a 5:1 activity concentration ratio compared to the surrounding cylinder. A measurement of the room background with the source removed was obtained on day 10. It was assumed that this background was constant in intensity and so could be subtracted (after proper acquisition-time scaling) from the count rates on all of the days. Since the measurements were carried out after hours when patients were no longer being imaged and since no high-energy sources are stored near the imaging site, this assumption is probably good.

The first camera, the Picker Prism 3000 XP, had settings for the energy windows that all involved 20% widths. The photopeak windows, which were visually centered on the first day, were located at indicated energies of 357, 372, and 378 keV for heads 1–3. The lower-energy windows, which we will call monitor windows, were placed just below the photopeak windows without overlapping them and were located at indicated energies of 291, 303, and 309 keV, respectively. The energy spectrum and the windows for head 2 of the Picker camera are shown in Fig. 1.

For both cameras, a standard clinical quality-control procedure (based on peaking for ^{99m}Tc) was being followed during the experimental measurements. This procedure adjusts camera high voltage to correct for electronic drift. We chose to use the same ^{131}I window settings for each measurement. We, therefore, are assuming both good quality control and also stability in the position of the ^{131}I peak relative to that of ^{99m}Tc over the time period. The advantage of this experimental procedure is its simplicity and its identity for both cameras.

The phantom was reproducibly placed on the headrest of the patient table with the lip over the edge, leaving the axis of the cylinder parallel to the axis of rotation. The table itself was reproducibly located within the gantry. Initially, head 1 was located directly below the phantom, as shown in Fig. 2. Data from all three heads were acquired. Then the camera was rotated 120° and a second acquisition obtained. This procedure was then repeated one final time. In this way, data was obtained for each head viewing the phantom from each of three angles.

The second camera, the two-headed Siemens Multispect, had windows that were originally located using the autopeak feature of the ICON™ MS-2 software and then, as with the Picker camera, kept the same. Again, good quality control and relative-peak-location stability are being assumed. As a result of the initial autopeaking, for both heads a 20% wide

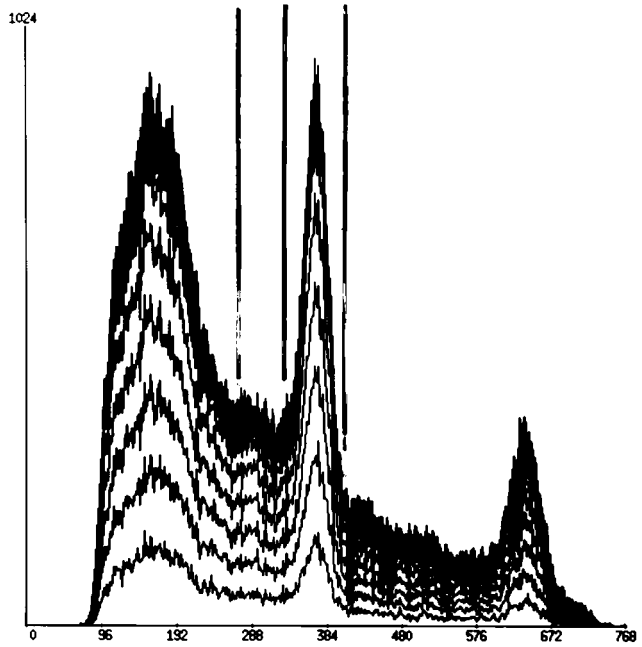

FIG. 1. Energy spectrum from the ^{131}I phantom for head 2 of the Picker camera. Counts are plotted against energy in keV. The pair of vertical lines toward the right denotes photopeak acceptance window while the pair toward the left denotes monitor window. Shorter peak at far right is 637 keV emission.

window was centered on the 364 keV photopeak and a 20% window centered at 287 keV for head 1 and at 292 keV for head 2 and, therefore, not quite contiguous to the photopeak window, were used for the monitor window.

The phantom was placed at the top of the patient couch with the pad removed and over the edge as for the Picker camera. Attention was again given to reproducible placement of the phantom and of the table. For this camera, head 2 was below the table and head 1 above. No rotation of the camera was carried out. Imaging times were the same as with the first camera and a background measurement was similarly made.

To begin the data analysis, the total number of counts in each projection was assessed. The background total count was weighted appropriately by the relative imaging time and subtracted. The result was divided by the image acquisition time on the particular day to provide count rates for the plots. To examine the deadtime appropriate for focal activity, a square ROI was placed over the circular image of a sphere. The size was kept constant throughout at 18×18 pixels. The location was determined visually but with a side condition of searching for the maximum number of counts. When the ROI was found for one of the two spheres for the photopeak window on one of the days, it was used in the same location for the monitor window. The background was also evaluated for these ROI and subtracted to obtain the sphere counts, except that it was so low with the Siemen's camera that it was ignored as negligible.

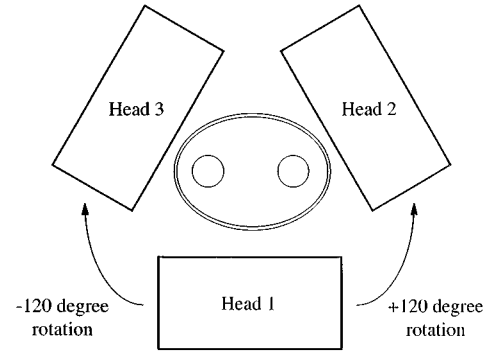

FIG. 2. Sketch of the phantom in place for a 0° acquisition by head 1 of the Picker Prism camera.

In processing, the results from the Picker camera, we computed a dead time constant by averaging over the three values measured at different angles to obtain a single value, t_a. At the maximum count rate, we also estimated the error in the dead time correction factor at each of the three angles due to using this average dead time constant. The procedure was to use the average constant and the measured count rate and solve Eq. (4) for F_a:

$$F_a = e^{N'\tau_a F_a}. \tag{5}$$

Then repeat the calculation with the measured constant at each angle, θ, to obtain $F_m(\theta)$:

$$F_m(\theta) = e^{N'\tau(\theta)F_m(\theta)}. \tag{6}$$

Next, calculate the error at each angle, $E(\theta)$, in percent from using the average value:

$$E(\theta) = \frac{[F_a - F_m(\theta)]}{F_m(\theta)} * 100\%. \tag{7}$$

We also compared the deadtime correction factor for the focal-activity count rate, F_{focal}, to the deadtime correction factor for the total image, F_{total}, and computed a fractional difference, D, as follows:

$$D = \frac{F_{\text{total}} - F_{\text{focal}}}{0.5*(F_{\text{total}} + F_{\text{focal}})} * 100\%. \tag{8}$$

This fractional difference will be negative if counts are being misplaced outside the spheres but still within the image.

Subsequent to the main experiment detailed above, testing of the camera heads was carried out to characterize the stability of the ^{131}I peak relative to that of ^{99m}Tc. A scatter-free source was reproducibly placed over each crystal after the collimator was removed. The location of the ^{131}I peak channel was checked seven times over 21 days by the Picker camera's standard software. On each occasion, five measurements were made for each head so that we could check the uncertainty of the location of the peak as determined by the

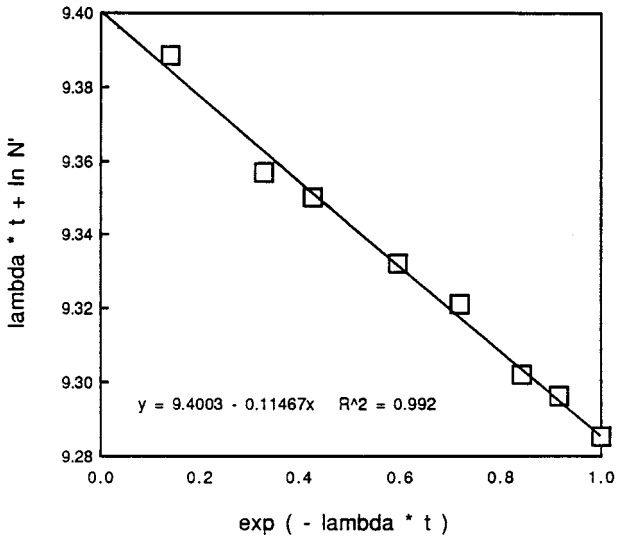

FIG. 3. The plot of the model fit with the best value for the square of the correlation coefficient among all the final results. Shown are results for the Picker Prism camera, head 1, for the photopeak window.

peak channel. For the Siemens camera, autopeaking was carried out seven times over 21 days. The off-peak shift from the target value (called the ''preset'') was recorded for each head.

IV. RESULTS

A. Deadtime constants

A plot of the data from the photopeak window for head 1 of the Picker camera positioned below the phantom (0°) is shown in Fig. 3. An excellent fit to the model is obtained with the square of the correlation value equal to 0.992. Similarly good fits are obtained for both windows, all three angles, and all three heads. For the 18 fits, the squared correlation constant averages 0.984 with a range of 0.960 to 0.992. The very good fits are consistent with good effective energy gain stability during the time of measurement.

The effect on the deadtime constant of object geometry is shown in Fig. 4. The constant is highest when the phantom is viewed face on at 0° and is lower when it is viewed obliquely by rotating the camera either $+120°$ or $-120°$. This fact is true for all three heads and for both of the windows. There is fairly good agreement between the symmetric geometries.

Table I shows the deadtime constant averaged over the three angles for each head and for each window. This average value is recommended for use in obtaining the deadtime correction for patients. By assuming the agreement between symmetric geometries should be perfect, one can obtain an estimate of the accuracy of the deadtime constant for a given geometry. That is, the difference in the deadtime constant between the two symmetrical geometries is calculated for each head and each window. The difference is averaged over the three heads. The resultant value of 0.15 μs for the photopeak window and 0.23 μs for the monitor window is a conservative error estimate for the respective average deadtime constants given in Table I.

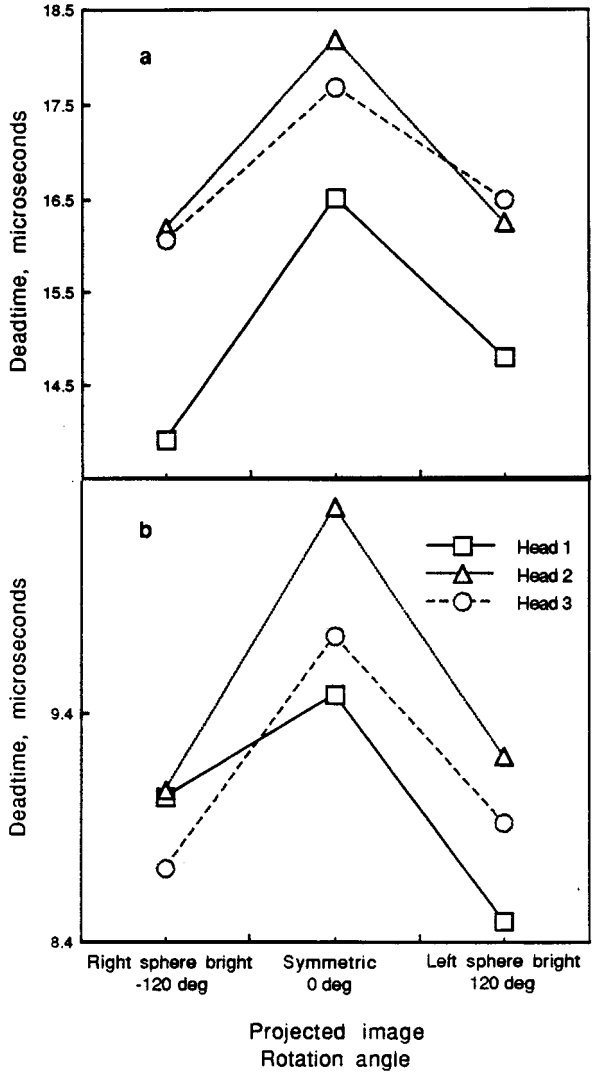

FIG. 4. The effect of the phantom geometry on the deadtime constant for each head and both windows of the Picker Prism camera. It is seen that the constant is highest when the phantom is viewed ''face on'' (as it is for head 1 in the sketch of Fig. 2). A deadtime constant averaged over the three geometries is calculated for patient correction at any angle. The result is given in Table I.

For the Siemens camera, the fits to the data from individual windows are fairly poor, especially for head 1 and for

TABLE I. Deadtime constant in microseconds for each camera, head, and window (for the Siemens camera, data from the two windows has been combined so there is only one deadtime constant per head).

Head	Picker		Siemens
	Photopeak	Monitor	Combined
1	9.00	15.07	1.53
2	9.52	16.87	2.18
3	9.12	16.75	

TABLE II. Fit results for Siemens camera.

Window	Head	R^2	τ
Photopeak	1	0.87	3.24 μs
Photopeak	2	0.98	4.74
Monitor	1	0.24	1.85
Monitor	2	0.72	2.35
Combined	1	0.77	1.53
Combined	2	0.96	2.18

the monitor window. The values are given in Table II. The data appear very noisy rather than having a nonlinear dependence. To improve the fits, we tried combining the counts from the two windows and replotting the data. Results from this procedure are better and are also given in Table II. Also, the poorer fit with combined data, that for head 1, is shown in Fig. 5. We use the linear fits to the combined data as first approximations to the deadtime behavior of the camera. The resultant deadtimes are, therefore, included in Table I. The procedure for patients is to combine the count rates for the two windows to calculate a deadtime correction factor; then apply this factor to the data from each window. This procedure is carried out at each angle of a SPECT acquisition.

B. Deadtime correction factors

At the maximum count rate we measured (that is, on the first day of imaging), the deadtime correction factor calculated from the average deadtime constant (or deadtime constant) for each head and window (or window combination) is given in Table III. The count rate at this time for head 1 of the Picker camera, which is typical for all heads of both cameras, is 10 795 counts per second for the photopeak window and 5818 counts per second for the monitor window.

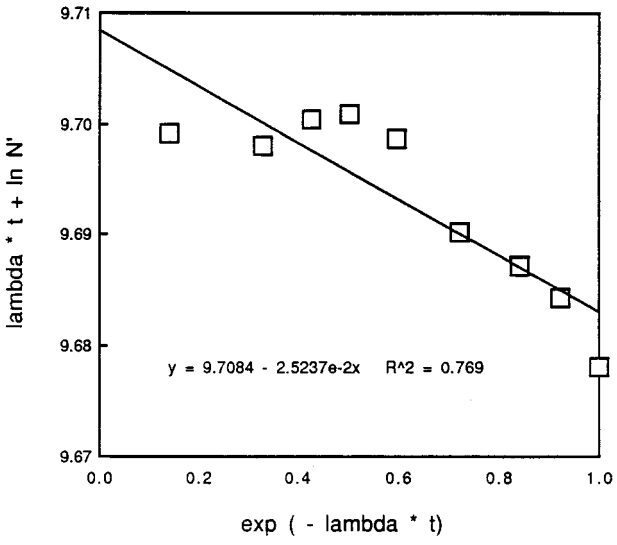

FIG. 5. A plot of the fit of the model that results in the worst value for the square of the correlation coefficient among all the total-image final results. Shown are the data for the Siemens camera, head 1, with the total-image counts for the photopeak and monitor windows combined.

TABLE III. Deadtime correction factor at maximum count rate.

	Picker		Siemens[a]
Head	Photopeak	Monitor	Combined
1	1.11	1.10	1.02
2	1.12	1.10	1.03
3	1.12	1.10	

[a]For the Siemens camera, data from the two windows has been combined so there is only one deadtime correction factor per head.

Table III shows that the Siemens camera has a much smaller deadtime correction factor, in general, and that the variation among heads (and between windows for the Picker camera) is small. The smallness of the correction with the Siemens camera to some extent justifies our use of a linear fit (even a large percentage error from the fit would not change the absolute value of the resultant correction by much).

C. Error from using average deadtime constant with Picker camera

At the maximum count rate with the Picker camera, the error, $E(\theta)$, from using the average deadtime constant ranges from -1.03% (for both the photopeak window with head 2 at 0° and the monitor window with head 1 at 0°) to $+0.79\%$ (for the monitor window with head 1 at $-120°$). The average of the absolute value of the percentage error is 0.55% ($n=18$). The smallness of the error in the deadtime correction factor justifies using the average value for the deadtime constant, in our opinion.

D. Deadtime for focal activity versus that for entire image

Fits to the data from the sphere ROI for the Picker camera at 0° were not as good as for the total-image data. The mean of the squared correlation coefficient for the 12 fits is 0.94, with a range of 0.88 to 0.98. The fits for the Siemens data were similarly more noisy with the mean of the squared correlation coefficient for the four fits equal to 0.66 with a range from 0.45 to 0.93. As in the case of the total image, head 1 fits were noisier than head 2 fits.

For the Picker camera at a maximum count rate, 11 out of 12 of the fractional differences, D, between focal and total-image correction-factor values are positive. The average fractional difference is $+1.68\%$ with a range of -0.62% to $+5.04\%$. These results tend to indicate a systematic difference between F_{focal} and F_{total}. However, the sign of the difference in the 11 cases is the opposite of what would be expected if counts were being misplaced between the two spheres. Since the mechanism of the difference is, therefore, unclear and since the average difference is less than 2%, we recommend the approach of using the total-image deadtime for correction.

For the Siemens camera, half the fractional differences, D, are positive and half negative. The average is $+0.23\%$ with a range of -1.47% to $+1.73\%$. For this camera with

an even split, there is no evidence of a systematic difference and so, again, we recommend using the total-image deadtime.

E. Relative stability of ^{131}I peak

For the Picker camera, the measured value for the peak channel had a standard deviation over 21 days (7 occasions) of 0.8 keV for head 1, 1.0 keV for head 2, and 0.7 keV for head 3. The uncertainty in the measurement of the location (the standard deviation of the mean for five individual measurements on each occasion) averaged 1.5 keV for head 1, 1.9 keV for head 2, and 1.6 keV for head 3. For each head, the uncertainty of the location is greater than the shift. For example, for head 1 1.5 keV is greater than 0.8 keV. Thus, there appears to be no verifiable relative shifting, and the assumption of good stability is validated.

For the Siemens camera, the result of repeated autopeaking for the photopeak had a standard deviation of 2.9 keV for head 1 and 1.8 keV for head 2. Assuming the ^{99m}Tc peak was being kept equally stable for the two cameras, there is more relative shifting with the Siemens camera than with the Picker camera. Making the assumption or not, one still concludes the effective energy gain stability with the Siemens camera is not quite as good as with the Picker camera.

V. DISCUSSION

Since we wanted one deadtime constant for each camera head involved, we have averaged multiple values from different angles where available. The resulting patient procedure would be to use the average constant in combination with the total count rate, which will vary with SPECT rotation angle, to obtain a deadtime correction factor for each angle of a SPECT acquisition. An alternative procedure would have been to interpolate between the three measured angles to obtain a deadtime constant as a function of angle. Since we had only three samples of the angular variation, and two were for redundant geometries, we have chosen not to follow this alternative. Fortunately, the deadtime correction factor varies somewhat slowly with the constant, and one will have the correct measured count rate. Moreover, no correction can be unbiased because we will already be making some error in the constant for any angle because the given patient will not match our phantom exactly.

Note that one could talk about the deadtime correction in terms of what fraction of the original data needs to be added to it to obtain the undistorted image. This fraction equals $F-1$. The errors and differences we have discussed could have been expressed as a percentage of this fraction. We would have then been discussing what percentage of the increment was in error. These percentages would have been about a factor of 10, i.e., $1/(1.10-1)$, larger. We would have been looking for the correction to be accurate rather than the total correction factor. By this tougher criterion, one might be less willing to accept the errors we have accepted. Our point of view is that we only need the final count rate to be good to, say, within 2% (and thus the correction factor) and that we do not need to hit the correction itself within 2%.

Judging by the pulse-height-analyzer display, the Siemens camera has a lower-energy upper-level discriminator than the Picker camera. This difference might be one source of the smaller deadtime correction factors for the Siemens camera with the same phantom. However, we choose not to conjecture on how much of a factor this might be.

Since the effective energy gain stability with the Siemens camera is not as good as with the Picker camera, employing autopeaking before each measurement might improve the fits to the paralyzable model, at least for the photopeak window. It also might be informative to check for changes in the shape of the energy spectra as the count rate changes. However, the means for this measurement are not readily at hand. From a practical point of view, since the maximum correction for our count range is only 3%, it is felt that further refinement of the correction is not necessary for our end goal of not contributing significantly to a quantitation uncertainty of 10% in activity determination.

VI. CONCLUSIONS

(1) At least up to moderately high count rates, the paralyzable model fits two current cameras operating in the ^{131}I dual-window-acquisition mode with fixed windows. For one of these cameras, however, it is necessary to combine data from the two windows and to calculate a single deadtime correction factor.

(2) In the case of the elliptical-cylinder source geometry, for the Picker camera, deadtime correction factors are similar for each head at the same count rate, and they are similar for the two windows. For the Siemens camera, the correction factor is also similar for the two heads at the same count rate and is smaller than for the Picker camera.

(3) For the Picker camera, there is a measurable dependence of the deadtime constant on source geometry for a given head and window.

(4) At our moderate count rates, for both cameras there is no indication that counts are being misplaced between focal activities at higher rates. For the Picker camera, there is some indication that the focal activity has a different deadtime correction factor than does the entire image. Since the average difference is only 2%, this unexplained effect needs further verification.

[1]K. F. Koral, K. R. Zasadny, M. L. Kessler, J-q. Luo, S. F. Buchbinder, M. S. Kaminski, I. Francis, and R. L. Wahl, ''CT-SPECT fusion plus conjugate views for determining dosimetry in I-131 - MoAb therapy of lymphoma patients,'' J. Nucl. Med. **35**, 1714–1720 (1994).

[2]K. F. Koral, F. M. Swailem, S. Buchbinder, N. H. Clinthorne, W. L. Rogers, and B. M. W. Tsui, ''SPECT dual-energy-window Compton correction: Scatter multiplier required for quantification,'' J. Nucl. Med. **31**, 90–98 (1990).

[3]K. R. Pollard, A. N. Bice, L. D. Durack, J. E. Eary, and T. K. Lewellen, ''Camera-induced Compton scatter and collimator penetration in iodine-131 imaging,'' J. Nucl. Med. **33**, 889 (1992) (abstract).

[4]K. R. Pollard, ''Correction for Compton scatter in iodine-131 gamma camera images, Ph.D. dissertaion, University of Washington, 1994.

[5]D. J. Macey, E. J. Grant, J. E. Bayouth, H. B. Giap, S. J. Danna, R. Sirisriro, and D. A. Podoloff, ''Improved conjugate view quantitation of I-131 by subtraction of scatter and septal penetration events with a triple energy window method,'' Med. Phys. **22**, 1637–1643 (1995).

[6]J. E. Eary, K. R. Pollard, L. D. Durack, A. N. Bice, T. K. Lewellen, D. Matthews, O. W. Press, W. B. Nelp, F. R. Appelbaum, and I. Bernstein, ''Post therapy imaging in high dose I-131 radioimmunotherapy patients,'' Med. Phys. **21**, 1157–1161 (1994).
[7]J. A. Sorenson, ''Deadtime characteristics of Anger cameras,'' J. Nucl. Med. **16**, 284–288 (1975).
[8]J. A. Sorenson, ''Methods of correcting Anger camera deadtime losses.'' J. Nucl. Med. **17**, 137–141 (1976).
[9]R. Adams, G. J. Hine, and C. D. Zimmerman, ''Deadtime measurements in scintillation cameras under scatter conditions simulating quantitative nuclear cardiography,'' J. Nucl. Med. **19**, 538–544 (1978).
[10]R. Wicks and M. Blau, ''The effect of window fraction on the deadtime of Anger cameras: Concise communication,'' J. Nucl. Med. **18**, 732–735 (1977).
[11]J. E. Arnold, A. S. Johnston, and S. M. Pinsky, ''The influence of true counting rate and the photopeak fraction of detected events on Anger camera deadtime,'' J. Nucl. Med. **15**, 412–416 (1974).
[12]K. Cranley, R. Millar, and T. K. Bell, ''Correction for deadtime losses in a gamma camera/data analysis system,'' Eur. J. Nucl. Med. **5**, 377–382 (1980).
[13]M. Ben-Porath, ''Camera deadtime: Rate-limiting factor in quantitative dynamic studies,'' Int. J. Nucl. Med. Biol. **2**, 107–112 (1975).
[14]R. Adams, C. Jansen, G. M. Grames, and C. D. Zimmerman, ''Deadtime of scintillation camera systems—definitions, measurement and applications,'' Med. Phys. **1**, 198–203 (1974).
[15]R. Adams and I. Mena, ''Testing the count rate performance of the scintillation camera by exponential attenuation: Decaying source; multiple filters,'' Med. Phys. **15**, 415–419 (1988).
[16]M. T. Madsen and R. J. Nickles, ''A precise method for correcting count-rate losses in scintillation cameras,'' Med. Phys. **13**, 344–349 (1986).
[17]A. N. Bice, K. R. Pollard, L. D. Durack, and W. B. Nelp, ''Comparative performance of methods for event loss estimation under conditions typical of radioimmunotherapy imaging,'' J. Nucl. Med. **33**, 1005–1006 (1992).
[18]K. R. Zasadny, K. F. Koral, and F. M. Swailem, ''Dead time of an anger camera in dual-energy-window-acquisition mode,'' Med. Phys. **20**, 1115–1120 (1993).
[19]C. Ceberg, I. Larsson, and S.-E. Strand, ''A new method for quantification of image distortion due to pile-up in scintillation cameras,'' Eur. J. Nucl. Med. **18**, 959–963 (1991).
[20]G. F. Knoll, *Radiation Detection and Measurement* (Wiley, New York, 1979), pp. 99–102.